Formation of Ultracold Heteronuclear Dimers in Electric Fields

Rosario González-Férez,[1,*] Michael Mayle,[2] and Peter Schmelcher[2,3]

[1] *Instituto 'Carlos I' de Física Teórica y Computacional and Departamento de Física Atómica Molecular y Nuclear, Universidad de Granada, E-18071 Granada, Spain*

[2] *Theoretische Chemie, Physikalisch–Chemisches Institut, Universität Heidelberg, Im Neuenheimer Feld 229, D-69120 Heidelberg, Germany*

[3] *Physikalisches Institut, Universität Heidelberg, Philosophenweg 12, D-69120 Heidelberg, Germany*

(Dated: February 1, 2008)

The formation of ultracold molecules via stimulated emission followed by a radiative deexcitation cascade in the presence of a static electric field is investigated. By analyzing the corresponding cross sections, we demonstrate the possibility to populate the lowest rotational excitations via photoassociation. The modification of the radiative cascade due to the electric field leads to narrow rotational state distributions in the vibrational ground state. External fields might therefore represent an additional valuable tool towards the ultimate goal of quantum state preparation of molecules.

PACS numbers: 33.80.Ps, 33.55.Be, 33.70.Ca

Over the past decade investigations of ultracold quantum gases have been revealing a wealth of intriguing phenomena. In particular, ultracold molecular systems represent a paradigm including molecular Bose-Einstein condensates [1, 2, 3]. External fields are equally important for the preparation and control of ultracold systems. They are used for cooling and trapping as well as for quantum state preparation or the tuning of atomic/molecular interactions, e.g., via Feshbach resonances [4, 5]. Moreover, they provide a tool to manipulate chemical reactions and collisions [6, 7], collisional spin relaxation in cold molecules [8], and rovibrational spectra and transitions [9, 10]. The quest for ultracold molecules being prepared in well-defined rovibrational quantum states is motivated by major perspectives such as the creation of quantum gases with novel many-body properties, ultracold state-to-state chemical reaction dynamics, or molecular quantum computation [11, 12, 13].

A special focus is the study of heteronuclear polar dimers and the possibility to create dipolar quantum gases [14]. Due to the permanent electric dipole moments of the constituent molecules, the intermolecular interaction becomes long-ranged thereby introducing exceptional properties for, e.g., the corresponding quantum gases. Electric fields play here an important role due to their immediate impact on polar systems which leads to rotational orientation and alignment of the molecules. The control of the formation process of ultracold polar molecules is a key issue to arrive at molecular quantum gases. Photoassociation of ultracold atoms is a widespread technique to produce ultracold molecules [15]. Indeed, the formation via photoassociation of KRb [16], LiCs [17], NaCs [18] and RbCs [19, 20] has been reported recently.

Let us consider a mixture of two atomic species in their electronic ground states, exposed to a linearly polarized laser with a frequency corresponding to the transition from the continuum to a highly excited vibrational bound state of the electronic ground state. The corresponding process of stimulated emission of a single photon allows for the formation of a polar molecule, see fig. 1 (note that hyperfine states are not considered). It has been recently studied for the LiH and NaH molecules [21, 22] focusing on the ultracold regime where $s \rightarrow p$-wave transitions dominate and only rovibrational bound states with angular momentum equal to one can be produced. Subsequently, a radiative cascade of rovibrational transitions leads to the vibrational ground state, thereby populating a broad range of rotational molecular states.

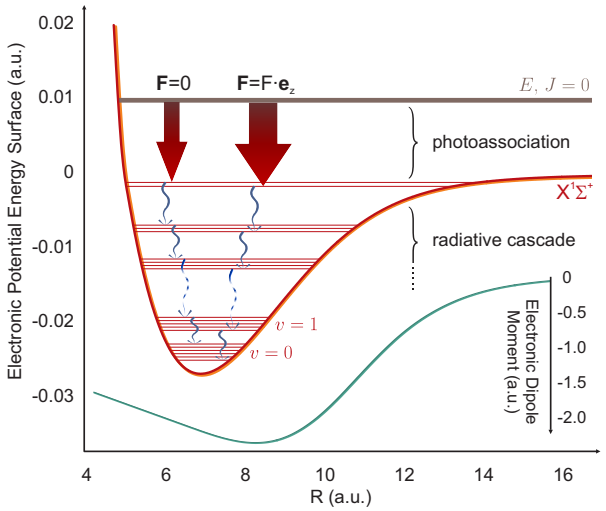

FIG. 1: (Color online) Electronic potential energy curve and dipole moment function of the electronic ground state $X\,^1\Sigma^+$ of the LiCs molecule, in atomic units. The schematics of the OPA and RDC are also shown (not to scale).

In the present work we explore the impact of an additional homogeneous static electric field on the formation process of polar dimers. As indicated above, the latter consists of the one-photon stimulated association (OPA) followed by a radiative deexcitation cascade (RDC). We

demonstrate that the presence of the static field allows one to populate via the OPA electrically dressed states evolving from field-free levels with zero angular momentum. This in combination with the following RDC yields a final rotational state distribution within the lowest vibrational band which is significantly narrower compared to the field-free case. Consequently, a static electric field can serve as a tool to prepare a molecular gas with only a limited number of well-defined molecular quantum states being populated. This might be a helpful step towards the goal of reaching quantum gases of molecules in their rovibrational ground states.

Let us assume that perturbation theory suffices for the description of the interaction with the laser field and for the interaction of the electronic motion with the static electric field. However, a nonperturbative treatment is indispensable for the impact of the electric field on the nuclear dynamics. The Hamiltonian for the rovibrational motion of the diatomic system in the Born-Oppenheimer approximation reads

$$H = -\frac{\hbar^2}{2\mu R^2}\frac{\partial}{\partial R}\left(R^2\frac{\partial}{\partial R}\right)+\frac{\mathbf{J}^2(\theta,\phi)}{2\mu R^2}+\varepsilon(R)-FD(R)\cos\theta \tag{1}$$

where the molecule fixed frame with the origin at the center of mass of the nuclei has been employed. (R,θ,ϕ) are the internuclear distance and the Euler angles, respectively. μ, $\mathbf{J}(\theta,\phi)$, $\varepsilon(R)$, F, and $D(R)$ are the reduced mass of the nuclei, the rotational angular momentum, the field-free electronic potential energy curve, the electric field strength, and the electronic dipole moment function, respectively. The electric field is parallel to the z-axis of the laboratory frame. In field-free space, each bound state of the molecule is characterized by its vibrational, rotational, and magnetic quantum numbers (v,J,M). In the presence of the electric field only the magnetic quantum number M is conserved. However, for reasons of addressability we will refer to the electrically dressed states by means of the corresponding field-free quantum numbers.

In the framework of the dipole approximation, the cross section of the stimulated emission process from the continuum $\Psi_E(\mathbf{R})$ to the rovibrational state $\Psi_\alpha(\mathbf{R})$ is given by

$$\sigma = \frac{\pi(E-E_\alpha)}{\hbar c\epsilon_0}|\langle\Psi_E|D(R)\cos\theta|\Psi_\alpha\rangle|^2 \tag{2}$$

where α labels the bound state and E, E_α are the continuum and rovibrational energies, respectively. The continuum wavefunctions are energy normalized while the rovibrational ones are $\mathcal{L}^2$ normalized.

The nuclear equation of motion associated with the Hamiltonian (1) is solved by means of a hybrid computational approach together with a Krylov-type diagonalization technique [23]. For the vibrational coordinate we use a mapped discrete variable representation based on sine functions [24] in a box of size L. A basis set expansion in terms of the associated Legendre functions is performed for the angular coordinate. This computational technique provides an accurate description of highly excited bound states, while the continuum spectrum is discretized and described by $\mathcal{L}^2$ normalized states. We emphasize that the traditional technique to represent energy normalized continuum wave functions by means of $\mathcal{L}^2$ normalized functions [25] is here not applicable due to the field-induced coupling between the rotational and vibrational motions. Moreover, the coupling significantly alters the definition of the density of continuum states. This issue has been solved by employing the time-dependent formalism. Since our study focuses on the ultracold regime with temperatures below 1 mK, very large discretization boxes are required to properly describe the continuum.

Being a topical example, we focus on the polar alkali dimer LiCs. The potential energy curve of its $X\,^1\Sigma^+$ electronic ground state is taken from experimental data [26] and the electric dipole moment function from semi-empirical calculations [27] (see fig. 1). Continuum energies corresponding to $T = 10, 100, 500\,\mu$K are considered. We analyze the stimulated emission process for the population of the rovibrational levels $(44,J,0)$, which is a reasonable but robust choice, with $J = 0, 1$, requiring laser wavelengths of $181.13\,\mu$m and $181.56\,\mu$m, respectively. Similar results are obtained for neighbouring vibrational bands. The dependence of the total cross sections on the electric field strength is shown in fig. 2. It is worth noting that the considered regime of field strengths covers the experimentally accessible range and beyond: Static fields $F > 4\cdot10^{-5}$ a.u. $= 200$ kV/cm are difficult to achieve in the laboratory. The cross sections increase with increasing temperature due to a larger overlap between the continuum and bound states. In the absence of the electric field, the ultracold regime is dominated by $s \to p$-wave transitions and the cross section for populating the $(44,0,0)$ state via the OPA process is several orders of magnitude smaller than the corresponding cross section involving the $(44,1,0)$ state.

Augmenting the field strength, the cross sections change significantly which can be explained by the hybridization of the angular motion. For $F \gtrsim 3\cdot10^{-6}$ a.u., the cross section for the $(44,0,0)$ state becomes larger than the one belonging to the $(44,1,0)$ state. Adopting $T = 10\,\mu$K, the cross section of the $J = 0$ state increases monotonically by two orders of magnitude within the regime $F = 10^{-7} - 10^{-5}$ a.u. Further increasing the field strength, it exhibits a plateau followed by a weakly pronounced minimum and a strong increase thereafter. In contrast to this, the cross section of the $(44,1,0)$ state shows a plateau in the weak field regime. For stronger fields it rapidly decreases and reaches a deep minimum for $F = 1.1\cdot10^{-5}$ a.u., followed by a broad maximum and a significant decrease for strong fields. This behaviour of

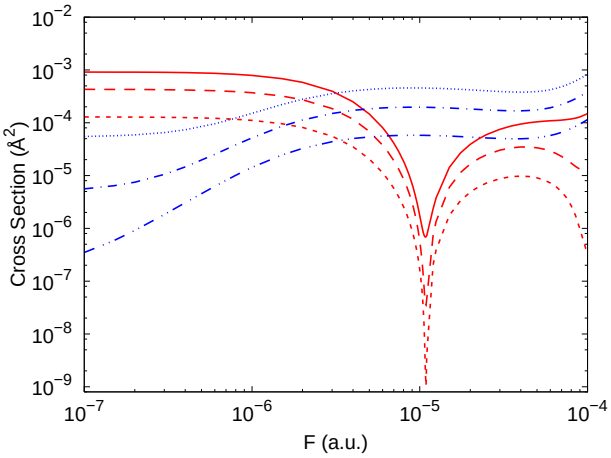

FIG. 2: (Color online) Stimulated emission cross sections as a function of the electric field strength for the states emerging from field-free levels with quantum numbers $(44,0,0)$ (dotted, dotted-dashed and double dotted-dashed lines) and $(44,1,0)$ (solid, dashed and short dashed lines) for continuum energies corresponding to $T = 500$, 100 and 10 μK, respectively.

the cross sections is due to the dominance of $s \rightarrow p$-wave transitions in the ultracold regime combined with the hybridization of the angular motion of the rovibrational state. Indeed, the presence of the plateaus in both cross sections is accompanied by an analogous constancy of the contribution of the p-wave to the corresponding wave functions. Similarly, the minimum for the $J = 1$ state at $F = 1.1 \cdot 10^{-5}$ a.u. is due to the dominance of s, d, and f-waves along with a rather weak contribution of the p-wave.

Let us shortly analyze the hybridization of the angular motion for these two states in more detail. The (44,0,0) state has a high-field-seeking character with an increasing expectation value $\langle \mathbf{J}^2 \rangle$ for augmenting fields, i.e., the contribution of higher field-free rotational states becomes larger as the electric field strength is enhanced. Consequently, this level shows a pronounced angular momentum hybridization $\mathbf{J}^2_h(44,0,0) = \langle \mathbf{J}^2 \rangle_{(44,0,0)} - J(J+1) =$ 2.08 and 7.88, for $F = 10^{-5}$ a.u. and 10^{-4} a.u., respectively, with J being the corresponding field-free rotational quantum number. On the other hand, the $(44,1,0)$ state shows initially a low-field-seeking behaviour where the admixing of lower rotations dominates and $\langle \mathbf{J}^2 \rangle$ decreases: $\mathbf{J}^2_h(44,1,0) = -0.11$ for $F = 10^{-6}$ a.u. Further enhancing the electric field, this level becomes a high-field-seeker, and $\langle \mathbf{J}^2 \rangle$ increases after reaching a minimum. In the strong field regime, this level exhibits a very pronounced hybridization $\mathbf{J}^2_h(44,1,0) = 21.45$ for $F = 10^{-4}$ a.u.

The formation rates in the OPA process can be varied significantly by simply changing the intensity of the applied laser. Specifically, if we assume an atomic density $n = 10^{12}$ cm^{-3}, a volume $V = 10^{-6}$ cm^3 illuminated by a laser beam with intensity 1 $\frac{\mathrm{kW}}{\mathrm{cm}^2}$, and a temperature $T = 1$ mK we obtain a formation rate of 10^4 molecules per second. Recently, the formation of LiCs molecules in a two-species magneto-optical trap by a two-photon process has been reported [17]. The molecules are formed in the electronic ground state, but an analysis of the final vibrational state distribution is not provided. With densities of 10^{10} cm^{-3} and $5 \cdot 10^9$ cm^{-3} for the Li and Cs atoms, respectively, and assuming a temperature of 100 μK, a molecular production rate between 1.4 ± 0.8 and 140 ± 80 molecules per second is estimated. Using these densities for the Li and Cs atoms, our theoretical results for the molecular formation rate via the OPA process are in the same order of magnitude. The reverse process of one photon absorption leading to the dissociation of the molecules is suppressed by the RDC (see below), although this is much more pronounced for light hydrides [21] compared to alkali dimers. It might be further eliminated by applying (chirped) laser pulses. Effects due to vibrational quenching can be neglected for not too large molecular densities.

Since the photoassociation process results in vibrationally highly excited states, a cascade of spontaneous emission processes will follow. The overall transition probability per unit time reads $\Gamma_\alpha = \sum_{v'J'M'}^{E_{\alpha'}<E_\alpha} \Gamma_{\alpha,\alpha'}$ where the summation includes all open decay channels, i.e., final levels α' with $M' \in \{M, M \pm 1\}$. The corresponding transition rates are

$$\Gamma_{\alpha,\alpha'} = \frac{\omega^3_{\alpha,\alpha'}}{3\pi\epsilon_0\hbar c^3} |\langle \Psi_\alpha | D(R) f_{M'}(\theta) | \Psi_{\alpha'} \rangle|^2 \qquad (3)$$

with $f_M(\theta) = \cos\theta$ and $f_{M\pm1}(\theta) = \sin\theta$. $\hbar\omega_{\alpha,\alpha'}$ is the energy difference between the initial and final states. The total and single-channel radiative lifetimes are $\tau_\alpha = (\Gamma_\alpha)^{-1}$ and $\tau_{\alpha,\alpha'} = (\Gamma_{\alpha,\alpha'})^{-1}$, respectively. Our aim is to analyze the final rotational state distribution in the lowest vibrational band resulting from the RDC. Starting from an initial state we therefore add up all decay paths resulting in a specific final state. This provides us the final J, M-state distributions.

Besides the possibility to form molecules evolving from field-free states with zero angular momentum by applying an electric field, the field interaction significantly alters the radiative properties of the bound molecular states. The rotational state distribution with varying (J, M) in the ground vibrational state which results from the radiation cascade of the $(44,1,0)$ state in the absence of the field is illustrated in fig. 3. The inset shows the cumulative population for fixed rotational quantum numbers J ($|M| \leq J$). Analogous results for the initial state $\alpha_0 = (44,0,0)$, but for $F = 4 \cdot 10^{-5}$ a.u., are presented in fig. 4. It should be noted that negative magnetic quantum numbers obey the same distribution due to the degeneracy of $\pm M$ states and the initial value $M = 0$. Augmenting the field from zero to $F = 4 \cdot 10^{-5}$ a.u., corresponding to 200$\frac{\mathrm{kV}}{\mathrm{cm}}$, the radiative lifetime of the $(44,0,0)$

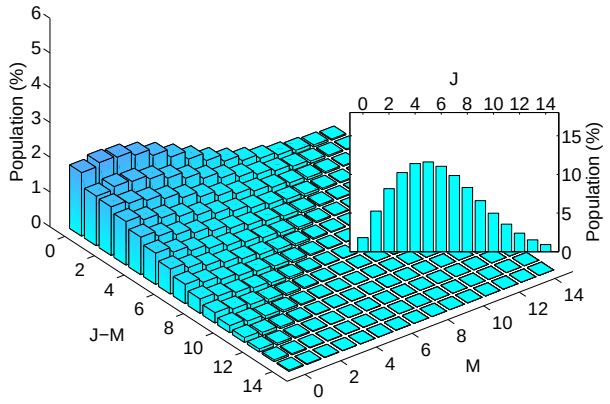

FIG. 3: (Color online) Population distribution as a function of the magnetic quantum number M and the difference $J-M$ for the decay cascade starting from the $(44,1,0)$ state in the absence of the electric field. The inset shows the cumulative population for fixed rotational quantum numbers.

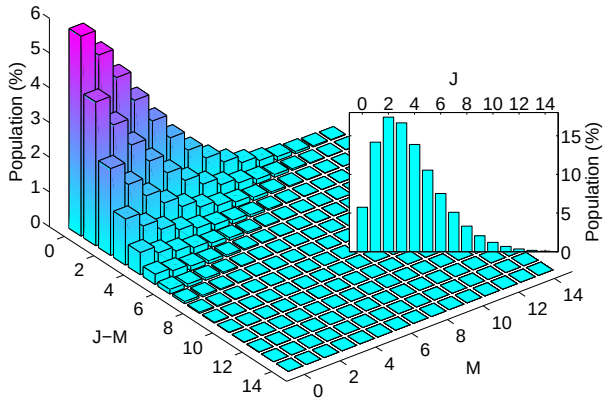

FIG. 4: (Color online) Same as in fig. 3 but with $(44,0,0)$ as initial state and for $F = 4\cdot 10^{-5}$ a.u.

state increases from 1.57 s to 2.15 s, while for the $(44,1,0)$ state it is reduced from 1.87 to 1.76 s. In both cases, the prevailing variation of the vibrational quantum number for each transition changes throughout the cascade from $\Delta v = 6$ for the $v = 44$ state to $\Delta v = 1$ for low-lying vibrational states. It is important to note that, in contrast to its favourable large electric dipole moment, LiCs represents a molecule with quite long radiative decay times. In comparison, heavier alkali dimers have even longer lifetimes, e.g., kiloseconds for the KRb molecule [28] while light hydrides such as LiH exhibit much shorter lifetimes of the order of a few milliseconds [21].

In the absence of the field, the selection rules $\Delta J = \pm 1$, $\Delta M \in \{0, \pm 1\}$ for dipole transitions hold, giving rise to a very broad distribution of the population in the lowest vibrational band: a large number of states exhibit a similar population. For a fixed J, the fully angular-momentum-polarized states always possess the largest population, and for fixed M the population slowly decreases with increasing J. Moreover, the two fastest paths populate the rotationally highly excited $(0, 20, \pm 20)$ states in 159 s. The cumulative population of the rotational bands exhibits a broad distribution with a maximum at $J = 5$. Similar results are obtained for the $(44,0,0)$ state. Once the vibrational ground state is populated, the rotational cascade is an extremely slow process: The lifetimes of the $(0,1,\pm 1)$ and $(0,5,\pm 5)$ levels are $1.88\cdot 10^6$ s and $1.1\cdot 10^4$ s, respectively. We remark that heating due to the random direction of the emitted photons in the course of the RDC is a minor effect amounting to several tens of nanokelvins for a typical setup [21].

The population of the final rotational states in the lowest vibrational band following the OPA and RDC changes drastically in the presence of the electric field. Due to the hybridization of the angular motion, only the selection rule $\Delta M \in \{0, \pm 1\}$ for the magnetic quantum number holds and many new transitions are possible. In particular, for fully polarized angular momentum states the importance of purely vibrational transitions $\Delta J = \Delta M = 0$ increases with increasing field strength and these transitions become dominant in the strong field regime [10]. Consequently, the distribution is much narrower and exhibits pronounced peaks for a few fully angular-momentum-polarized states as can be seen by comparing figs. 3 and 4. For $F = 4\cdot 10^{-5}$ a.u., the RDC is dominated by these purely vibrational transitions and the rovibrational ground state possesses the largest population of 5.75 % compared to 2.02 % for $F = 0$. This effect can be further enhanced by employing even higher fields. In addition, the rovibrational ground state is populated by the most probable paths. Accordingly, we observe in the inset of fig. 4 that the maximum of the cumulative rotational state population is shifted to the $J = 2$ band and includes 17.4% of the overall norm. The entire RDC process to the vibrational ground state typically takes several minutes. We remark that the subsequent rotational decay itself is enhanced significantly in the presence of the field and the corresponding fully angular-momentum-polarized states possess a unique radiative decay route to the rovibrational ground state [10].

The above analysis demonstrates that the formation of ultracold molecules in their electronic ground state via a single-photon stimulated emission process followed by a radiative cascade can be significantly altered by the presence of a static electric field. The resulting narrow rotational distributions in the lowest vibrational band represent a remarkable step towards the ultimate goal of degenerate quantum gases of molecules in their rovibrational ground state, or more generally in any desired unique quantum state. Although our study focuses on the LiCs molecule, a qualitatively similar behaviour has to be expected for other heteronuclear dimers depending

on the corresponding potential energy curve and electric dipole moment function.

R.G.F. acknowledges the support of the Junta de Andalucía under the program of Retorno de Investigadores a Centros de Investigación Andaluces. Financial support by the Acciones Integradas Hispano Alemanas HA2005–0038 (MEC and DAAD) and of the Spanish projects FIS2005–00973 (MEC) as well as FQM–0207 and FQM–481 (Junta de Andalucía) is gratefully appreciated. We thank particularly Hans-Dieter Meyer for his strong support concerning the workout of the time-dependent formalism. Roland Wester is acknowledged for fruitful discussions, Peter Staanum for providing us with the potential energy curve, and Olivier Dulieu for the electric dipole moment of the LiCs molecule.

* Electronic address: rogonzal@ugr.es

[1] S. Jochim *et al.*, Science **302**, 2101 (2003).
[2] M. Greiner, C. A. Regal, and D. S. Jin, Nature **426**, 537 (2003).
[3] M. W. Zwierlein *et al.*, Phys. Rev. Lett. **91**, 250401 (2003).
[4] C. Wieman, D. E. Pritchard, and D. Wineland, Rev. Mod. Phys. **71**, S253 (1999).
[5] C. Pethick and H. Smith, Bose-Einstein Condensation in Dilute Gases, Cambridge University Press (2002).
[6] R. V. Krems, Int. Rev. Phys. Chem. **24**, 99 (2005).
[7] R. V. Krems, Phys. Rev. Lett. **96**, 123202 (2006).
[8] T. V. Tscherbul and R. V. Krems, Phys. Rev. Lett. **97**, 083201 (2006).
[9] R. González-Férez, M. Mayle, and P. Schmelcher, Chem. Phys. **329**, 203 (2006).
[10] M. Mayle, R. González-Férez, and P. Schmelcher, Phys. Rev. A **75**, 013421 (2007).
[11] D. DeMille, Phys. Rev. Lett. **88**, 067901 (2002).
[12] S. F. Yelin, K. Kirby, and R. Côté, Phys. Rev. A **74**, 050301(R) (2006).
[13] M. Weidemüller and C. Zimmermann, Eds., Interactions in Ultracold Gases, Wiley-VCH (2003).
[14] *Topical Issue on Ultracold Polar Molecules: Formation and Collisions*, Eur. Phys. J. D 31 (2004).
[15] K. M. Jones, E. Tiesinga, P. D. Lett, and P. S. Julienne, Rev. Mod. Phys. **78**, 483 (2006).
[16] D. Wang *et al.*, Eur. Phys. J. D **31**, 165 (2004).
[17] S. D. Kraft *et al.*, J. Phys. B **39**, S993 (2006).
[18] C. Haimberger, J. Kleinert, M. Bhattacharya, and N. P. Bigelow, Phys. Rev. A **70**, 021402(R) (2004).
[19] A. J. Kerman, J. M. Sage, S. Sainis, T. Bergeman, and D. DeMille, Phys. Rev. Lett. **92**, 153001 (2004).
[20] J. M. Sage, S. Sainis, T. Bergeman, and D. DeMille, Phys. Rev. Lett. **94**, 203001 (2005).
[21] E. Juarros, P. Pellegrini, K. Kirby, and R. Côté, Phys. Rev. A **73**, 041403(R) (2006).
[22] E. Juarros, K. Kirby, and R. Côté, J. Phys. B **39**, S965 (2006).
[23] R. B. Lehoucq, D. C. Sorensen, and C. Yang, *ARPACK User's Guide* (SIAM, Philadelphia, 1998).
[24] R. González-Férez and H.-D. Meyer, preprint 2006.
[25] E. Luc-Koenig, M. Vatasescu, and F. Masnou-Seeuws, Eur. Phys. J. D **31**, 239 (2004).
[26] P. Staanum, A. Pashov, H. Knoeckel, and E. Tiemann, physics/0612031 (2006).
[27] M. Aymar and O. Dulieu, J. Chem. Phys. **122**, 204302 (2005).
[28] W. T. Zemke and W. C. Stwalley, J. Chem. Phys. **120**, 88 (2004).